Graphene, 2015, 4, 75-83
Published Online October 2015 in SciRes. http://www.scirp.org/journal/graphene
http://dx.doi.org/10.4236/graphene.2015.44008

The Surface Reactivity of Pure and Monohydrogenated Nanocones Formed from Graphene Sheets

Ahlam A. El-Barbary[1,2*], Mohamed A. Kamel[1], Khaled M. Eid[1,3], Hayam O. Taha[1], Rasha A. Mohamed[1], Mohammed A. Al-Khateeb[1]

[1]Physics Department, Faculty of Education, Ain Shams University, Cairo, Egypt
[2]Physics Department, Faculty of Science, Jazan University, Jazan, KSA
[3]Bukairiayh for Science, Qassim University, Qassim, KSA
Email: *ahla_eg@yahoo.co.uk

Received 29 July 2015; accepted 6 September 2015; published 9 September 2015

Abstract

A systematic computational study of surface reactivity for pure and mono-hydrogenated carbon nanocoes (CNCs) formed from graphene sheets as functions of disclination angle, cone size and hydrogenation sites has been investigated through density functional (DFT) calculations and at the B3LYP/3-21G level of theory. Five disclination angles (60˚, 120˚, 180˚, 240˚ and 300˚) are applied and at any disclination angle four structures with different sizes are studied. For comparison, pure and mono-hydrogenated boron nitride nanocones (BNNCs) with disclination angles 60˚, 120˚, 180˚, 240˚ and 300˚ are also investigated. The hydrogenation is done on three different sites, H^{S1} (above the first neighbor atom of the apex atoms), H^{S2} (above one atom of the apex atoms) and H^{S3} (above one atom far from the apex atoms). Our calculations show that the highest surface reactivity for pure CNCs and BNNCs at disclination angles 60˚, 180˚ and 300˚ is 23.50 Debye for $B_{41}N_{49}H_{10}$ cone and at disclination angles 120˚ and 240˚ is 15.30 Debye for $C_{94}H_{14}$ cone. For mono-hydrogenated CNCs, the highest surface reactivity is 22.17 Debye for $C_{90}H_{10}$-H^{S3} cone at angle 300˚ and for mono-hydrogenated BNNCs the highest surface reactivity is 28.97 Debye for $B_{41}N_{49}H_{10}$-H^{S1} cone when the hydrogen atom is adsorbed on boron atom at cone angle 240˚.

Keywords

Carbon Nanocones, Boron Nitride Nanocones, DFT, Surface Reactivity, Hydrogenation

*Corresponding author.

How to cite this paper: El-Barbary, A.A., Kamel, M.A., Eid, K.M., Taha, H.O., Mohamed, R.A. and Al-Khateeb, M.A. (2015) The Surface Reactivity of Pure and Monohydrogenated Nanocones Formed from Graphene Sheets. *Graphene*, **4**, 75-83.
http://dx.doi.org/10.4236/graphene.2015.44008

1. Introduction

The hallow shape and the curvature of CNTs that are not present in bulk graphite make them easier to storage hydrogen inside and outside the tube surface. At the same line, one of the most important applications of CNCs (representing the fifth allotropic form of carbon) is hydrogen storage. Hydrogen storage on CNCs has been explored theoretically [1]-[10] and experimentally [11]-[13]. In addition, the fabrication of CNCs has attracted attention because of their mechanical stability and sharp tip structures [14] [15]. Also, CNCs can be used as practical phononic devices, scanning probe tips and electron field emitters [16]-[18]. The field emission properties of cone-shaped CNTs whose tip are stacked by CNCs have been investigated [19]. Furthermore, decorating the network of carbon nanostructures by nitrogen and boron has been studied [20]-[22]. The main problem of hydrogen storage is that a hydrogen fuel-cell must be of comparable weight and size to current gas tanks for the technology to gain acceptance where the determined hydrogen storage density of 9 wt% is required. Therefore, the main idea behind this work is to investigate the ability of CNCs and BNNCs for hydrogen storage via surface reactivity study. By increasing the surface reactivity, the ability of hydrogen storage is expected to be increased. To provide a better understanding of surface reactivity, pure CNCs and BNNCs, in addition to mono-hydrogenated CNCs and BNNCs are studied. Five disclination angles 60˚, 120˚, 180˚, 240˚ and 300˚ are applied on graphene sheet and the cones 60˚, cones 120˚, cones 180˚, cones 240˚ and cones 300˚ are obtained. At any disclination angle for CNCs and BNNCs, four structures with different sizes are studied in order to understand the effect of the size on the surface reactivity of NCs, except for BNNCs with disclination angles 60˚, 180˚ and 300˚ eight structures for each disclination angle are studied. Also, the hydrogenation is done on three different sites, H^{S1} (above the first neighbor atom of the apex atoms), H^{S2} (above one atom of the apex atoms) and H^{S3} (above one atom far from the apex atoms). Hopefully, these results could be useful for testing the capability of CNCs and BNNs as hydrogen storage systems.

2. Methodology

Density Functional Theory (DFT) calculations have been performed employing the B3LYP exchange-correlation functional [23] [24] and the 3-21G standard basis set as implemented in the Gaussian 03W program [25] [26]. The samples of study are pure and mono-hydrogenated CNCs and BNNCs with five disclination angles, 60˚ (a five-membered ring at the apex), 120˚ (a four-membered ring at the apex), 180˚ (a three-membered ring at the apex), 240˚ (a bicyclic system at the apex) and 300˚ (a complex with a three-membered and four-membered rings at the apex), see **Figure 1**. The hydrogenation is done on three different sites, H^{S1} (above the first neighbor

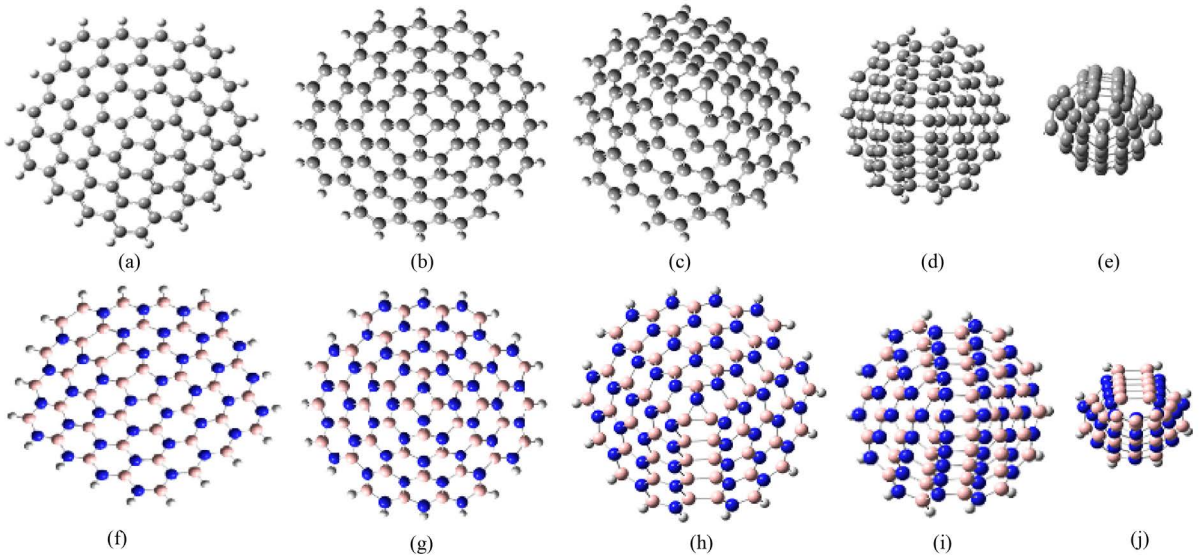

Figure 1. Optimized structures of CNCs and BNNCs: (a) and (f) cones 60˚, (b) and (g) cones 120˚, (c) and (h) cones 180˚, (d) and (i) cones 240˚, (e) and (j) cones 300˚. Grey atoms represent carbon atoms, blue atoms represent nitrogen atom and pink atoms represent boron atoms. Arrows refer to the bonds between connected atoms edges (boron atoms, model M2).

atom of the apex atoms), H^{S2} (above one atom of the apex atoms) and H^{S3} (above one atom far from the apex atoms). To avoid the dangling effects, the hydrogen atoms have been used to saturate the ending atoms for CNCs and BNNCs. All the atomic geometries of pure and mono-hydrogenated CNCs and BNNCs have been allowed to fully relaxation during the optimization processes.

3. Results

3.1. Geometric Structures of CNCs and BNNCs

The CNCs are consisting of curved graphite sheets formed as open cones and are constructed by cutting out sectors of n × 60˚ (n = 1 - 5) from the flat sheet of graphene and connecting the edges. In the present work, we have investigated cone 60˚ (a five-membered ring at the apex), cone 120˚ (a four-membered ring), cone 180˚ (a three-memberedring), cone 240˚ (a bicyclic system), and cone 300˚ (a complex with a three-membered and four-membered rings at the apex), see **Figures 1(a)-(e)**. At the same line the BNNCs are constructed, see **Figures 1(f)-(j)**. For all CNCs and BNNCs with disclination angles 120˚ and 240˚, there is only one model. However, for BNNCs with disclination angles 60˚, 180˚, and 300˚ there are two models (M1 and M2), resulting from the connected atoms edges can be either nitrogen atoms (named M1) or can be boron atoms (named M2).

3.2. Surface Reactivity of Pure CNCs and BNNCs

The surface reactivity of pure CNCs and BNNCs at different disclination angels n × 60˚ (n = 1 to 5) are studied. Also, at any disclination angle the effect of the cone size is tested through working on four different structures. By this way, one can test the effects of size, disclination angle and types of NCs on the surface reactivity of NCs.

The surface reactivity of CNCs and BNNCs at disclination angle 60˚ is investigated and is listed in **Table 1**. The dipole moments are calculated and are used as indicator for the surface reactivity [27] [28] where the high values of the dipole moments indicate the high surface reactivity and vice versa. As shown in **Table 1**, the surface reactivity of cone 60˚ is increased by increasing the cone size. Also, it found that the $B_{82}N_{87}H_{30}$ (M1) cone 60˚ possesses the highest surface reactivity (13.1 Debye), followed by $C_{169}H_{30}$ cone 60˚ (12.1 Debye) and the smallest surface reactivity is for $B_{87}N_{82}H_{30}$ (M2) cone 60˚ (7.1 Debye). In other words, by increasing the number of nitrogen atoms (in case of the type of connected atoms edges is nitrogen atoms) and decreasing the number of boron atoms, the surface reactivity of BNNCs is increased.

Table 2 shows the calculated surface reactivity of CNCs and BNNCs at disclination angle 120˚. It is found that the calculated surface reactivity of cones 120˚ is increased by increasing the cone size. Also, it is noticed that the surface reactivity of the $C_{136}H_{24}$ cone 120˚ (13.6 Debye) is higher than the surface reactivity of $B_{68}N_{68}H_{24}$ cones 120˚ (9.2 Debye). This indicates that when the number of boron atoms is equal to number of nitrogen atoms (*i.e*. type of connected atoms edges is both of nitrogen and boron atoms), the surface reactivity of BNNCs is reduced. From **Table 1** and **Table 2**, it is clear that by increasing the disclination angle (from cones 60˚ to cones 120˚), the surface reactivity is increased for both of CNCs and BNNCs.

The surface reactivity of CNCs and BNNCs at disclination angle 180˚ is listed in **Table 3**. As shown in **Table 3**, the surface reactivity of cones180˚ is increased by increasing the cone size. Also, it is found that the

Table 1. The configuration structures and the dipole moments of the CNCs 60˚ and BNNCs 60˚. The dipole moment is given by Debye.

Stoichiometry cones 60˚	N	M	Y	$C_{n+m}H_y$	$B_nN_mH_y$ M1	$B_mN_nH_y$ M2
				Dipole moment/Debye		
St1	21	24	15	5.4	7.2	4.9
St2	38	42	20	7.9	9.5	5.5
St3	56	59	25	9.2	9.8	6.6
St4	82	87	30	12.1	13.1	7.1

M1 refers to the type of connected atoms edges is nitrogen atoms, M2 refers to the type of connected atoms edges is boron atoms.

Table 2. The configuration structures and the dipole moments of the CNCs 120˚ and BNNCs 120˚. The dipole moment is given by Debye.

Stoichiometry cones 120˚	M	Y	$C_{2m}H_y$	$B_mN_mH_y$
			Dipole moment/Debye	
St1	18	12	6.1	5.1
St2	28	16	8.0	5.7
St3	46	20	10.7	7.5
St4	68	24	13.6	9.2

Table 3. The configuration structures and the dipole moments of the CNCs 180˚ and BNNCs 180˚. The dipole moment is given by Debye.

Stoichiometry cones 180˚	N	M	Y	$C_{n+m}H_y$	$B_nN_mH_y$ M1	$B_mN_nH_y$ M2
				Dipole moment/Debye		
St1	22	26	12	7.8	12.1	7.1
St2	35	40	15	9.3	13.1	8.9
St3	49	53	18	9.8	15.2	9.4
St4	68	73	21	11.5	15.9	11.2

$B_{68}N_{73}H_{21}$ (M1) cone 180˚ possesses the highest surface reactivity (15.9 Debye), followed by $C_{141}H_{21}$ cone 180˚ (11.5 Debye) and the smallest surface reactivity is for $B_{73}N_{68}H_{21}$ (M2) cone 180˚ (11.2 Debye). In addition, the surface reactivity of cones 180˚ is found to be higher than the surface reactivity of the cones 120˚ and the latter is higher than the cones 60˚.

From **Table 4**, the calculated surface reactivity of CNCs and BNNCs at disclination angle 240˚ is increased by increasing the cone size. Also, it is found that the surface reactivity of the $C_{94}H_{14}$ cone 240˚ (15.3 Debye) is higher than the surface reactivity of $B_{47}N_{47}H_{14}$ cone 240˚ (11.9 Debye). From **Tables 1-4**, it is clear that by increasing the disclination angle (from cones 60˚ to cones 240˚), the surface reactivity is increased.

The surface reactivity of CNCs and BNNCs at disclination angle 300˚ is shown in **Table 5**. It is found that the surface reactivity of cones 300˚ is increased by increasing the cone size. Also, it is found that the $B_{41}N_{49}H_{10}$ (M1) cone 300˚ possesses the highest surface reactivity (23.5 Debye), followed by $C_{90}H_{10}$ cone 300˚ (23.5 Debye) and the smallest surface reactivity is for $B_{49}N_{41}H_{10}$ (M2) cone 300˚ (12.5 Debye).

From **Tables 1-5**, one can report that the surface reactivity is increased by increasing the cone size and the disclination angle. In addition, the highest surface reactivity is for $B_nN_mH_y$ (M1) cones when the type of connected atoms edges is nitrogen atoms (at disclination angles 60˚, 180˚ and 300˚), otherwise the surface reactivity of $C_{2m}H_y$ cones is always higher than $B_mN_mH_y$ cones (at disclination angles 120˚ and 240˚).

3.3. Surface Reactivity of Mono-Hydrogenated CNCs and BNNCs

The surface reactivity of mono-hydrogenated CNCs at three different hydrogenation sites H^{S1} (above the first neighbor atom of the apex atoms), H^{S2} (above one atom of the apex atoms) and H^{S3} (above one atom far from the apex atoms) for each disclination angels n × 60˚ (n = 1 to 5) are studied, see **Figure 2**. Also, at any disclination angle the effect of the cone size is tested through working on four different structures. By this way, one can test the effects of size, disclination angle and hydrogenation site of CNCs on the surface reactivity of mono-hydrogenated CNCs. From **Table 6**, it is found that the surface reactivity of mono-hydrogenated CNCs is increased by increasing the size and dsiclination angles of CNCs. Also, the surface reactivity at hydrogenation site H^{S3} always possesses the highest dipole moment, followed by H^{S1} and H^{S2} sites. The highest surface reactivities at disclination angles 60˚, 120˚, 180˚, 240˚ and 300˚ are found to be 10.94 Debye for $C_{170}H_{30}$-H^{S1}, 12.58 Debye for $C_{136}H_{24}$-H^{S3}, 18.70 Debye for $C_{141}H_{21}$-H^{S1}, 16.98 Debye for $C_{94}H_{14}$-H^{S3} and 22.17 Debye for $C_{90}H_{10}$-H^{S3}, respectively. Finally, on can conclude that the best cone size, the best hydrogenation site and best disclination angle for hydrogen adsorption is for CNC $C_{90}H_{10}$-H^{S3} at 300˚ declination angle.

Table 4. The configuration structures and the dipole moments of the CNCs 240˚ and BNNCs 240˚. The dipole moment is given by Debye.

Stoichiometry cones 240˚	M	Y	$C_{2m}H_y$	$B_mN_mH_y$
			Dipole moment/Debye	
St1	14	8	8.0	7.9
St2	23	10	11.8	9.0
St3	34	12	12.0	10.0
St4	47	14	15.3	11.9

Table 5. The configuration structures and the dipole moments of the CNCs 300˚ and BNNCs 300˚. The dipole moment is given by Debye.

Stoichiometry cones 300˚	N	M	Y	$C_{n+m}H_y$	$B_nN_mH_y$ M1	$B_mN_nH_y$ M2
				Dipole moment/Debye		
St1	15	19	6	11.2	11.7	8.0
St2	21	26	7	12.8	13.4	10.4
St3	34	41	9	18.6	19.0	10.9
St4	41	49	10	21.9	23.5	12.5

Table 6. The configuration structures and the dipole moments of mono-hydrogenated CNCs. The dipole moment is given by Debye.

Angle 60˚		Angle 120˚		Angle 180˚		Angle 240˚		Angle 300˚	
Systems	*Dipole moment*	Systems	*Dipole moment*	Systems	*Dipole moment*	Systems	*Dipole moment*	Systems	*Dipole moment*
$C_{45}H_{15}$-H^{S1}	5.63	$C_{36}H_{12}$-H^{S1}	5.87	$C_{48}H_{12}$-H^{S1}	7.60	$C_{28}H_8$-H^{S1}	3.16	$C_{23}H_5$-H^{S1}	3.22
$C_{45}H_{15}$-H^{S2}	3.65	$C_{36}H_{12}$-H^{S2}	4.93	$C_{48}H_{12}$-H^{S2}	7.17	$C_{28}H_8$-H^{S2}	3.68	$C_{23}H_5$-H^{S2}	2.46
$C_{45}H_{15}$-H^{S3}	5.02	$C_{36}H_{12}$-H^{S3}	6.11	$C_{48}H_{12}$-H^{S3}	8.43	$C_{28}H_8$-H^{S3}	5.54	$C_{23}H_5$-H^{S3}	5.88
$C_{80}H_{20}$-H^{S1}	6.92	$C_{56}H_{16}$-H^{S1}	6.94	$C_{75}H_{15}$-H^{S1}	12.73	$C_{46}H_{10}$-H^{S1}	6.67	$C_{34}H_6$-H^{S1}	10.31
$C_{80}H_{20}$-H^{S2}	6.03	$C_{56}H_{16}$-H^{S2}	6.38	$C_{75}H_{15}$-H^{S2}	10.46	$C_{46}H_{10}$-H^{S2}	6.01	$C_{34}H_6$-H^{S2}	6.72
$C_{80}H_{20}$-H^{S3}	7.09	$C_{56}H_{16}$-H^{S3}	7.42	$C_{75}H_{15}$-H^{S3}	11.26	$C_{46}H_{10}$-H^{S3}	6.93	$C_{34}H_6$-H^{S3}	10.42
$C_{115}H_{25}$-H^{S1}	9.14	$C_{92}H_{20}$-H^{S1}	8.49	$C_{102}H_{18}$-H^{S1}	11.23	$C_{68}H_{12}$-H^{S1}	5.92	$C_{58}H_8$-H^{S1}	15.61
$C_{115}H_{25}$-H^{S2}	6.64	$C_{92}H_{20}$-H^{S2}	8.78	$C_{102}H_{18}$-H^{S2}	11.65	$C_{68}H_{12}$-H^{S2}	7.81	$C_{58}H_8$-H^{S2}	12.39
$C_{115}H_{25}$-H^{S3}	7.94	$C_{92}H_{20}$-H^{S3}	10.38	$C_{102}H_{18}$-H^{S3}	11.98	$C_{68}H_{12}$-H^{S3}	8.53	$C_{58}H_8$-H^{S3}	13.28
$C_{170}H_{30}$-H^{S1}	10.94	$C_{136}H_{24}$-H^{S1}	12.18	$C_{141}H_{21}$-H^{S1}	18.70	$C_{94}H_{14}$-H^{S1}	6.73	$C_{90}H_{10}$-H^{S1}	18.38
$C_{170}H_{30}$-H^{S2}	9.52	$C_{136}H_{24}$-H^{S2}	11.52	$C_{141}H_{21}$-H^{S2}	15.99	$C_{94}H_{14}$-H^{S2}	7.51	$C_{90}H_{10}$-H^{S2}	17.93
$C_{170}H_{30}$-H^{S3}	10.79	$C_{136}H_{24}$-H^{S3}	12.58	$C_{141}H_{21}$-H^{S3}	15.55	$C_{94}H_{14}$-H^{S3}	16.98	$C_{90}H_{10}$-H^{S3}	22.17

H^{S1} refers to the hydrogenation site is above the first neighbor atom of the apex atoms. H^{S2} refers to the hydrogenation site is above one atom of the apex atoms. H^{S3} refers to the hydrogenation site is above one atom far from the apex atoms.

Also, the surface reactivity of mono-hydrogenated BNNCs at three different hydrogenation sites H^{S1}, H^{S2} and H^{S3} for each disclination angels n × 60˚ (n = 1 to 5), are studied. The hydrogen atom can be adsorbed on boron atom (named Type1) or can be adsorbed on nitrogen atom (named Type2). As we mention above, for disclination angles 60˚, 180˚ and 300˚ there are two models of BNNCs, BNNCs-M1 (the connected edges atoms are nitrogen atoms) and BNNCs-M2 (the connected edges atoms are boron atoms). Therefore, for the surface reactivity of BNNCs at disclination angles 120˚ and 240˚ for there are two systems of BNNCs, BNNCs-Type1 and BNNCs-Type2, see **Table 6**. However, for disclination angles 60˚, 180˚ and 300˚ there are four systems of BNNCs, BNNCs-M1-Type1, BNNCs-M1-Type2, BNNCs-M2-type1 and BNNCs-M2-Type2, see **Table 7** and **Table 8**.

From **Table 7**, it is clear that the surface reactivities for monohydrogenated BNNCs-Type1 and BNNCs-Type2

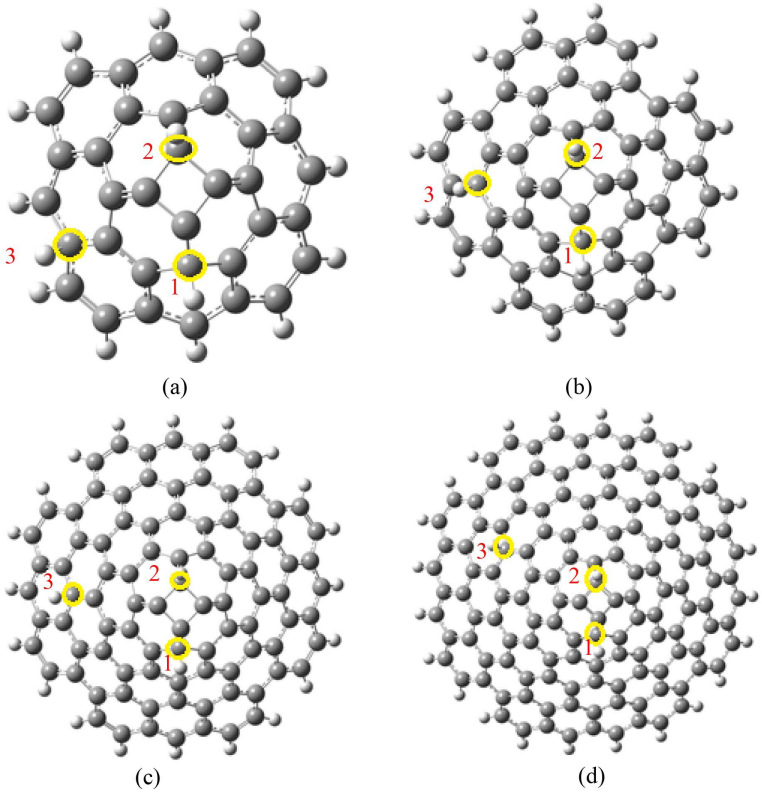

Figure 2. Schematic representation for hydrogenation sites 1-H^{S1}, 2-H^{S2}, 3-H^{S3} of CNCs with disclination angle 120˚ for structures (a) $C_{36}H_{12}$, (b) $C_{56}H_{16}$, (c) $C_{92}H_{20}$ and (d) $C_{136}H_{24}$. Circles refer to the hydrogenation sites.

are increased by increasing the cone size and cone angle. For disclination angle 120˚, the highest surface reactivates for Type1 and Type2 are found to be 10.90 Debye for $B_{68}N_{68}H_{24}$-H^{S2} and 11.75 Debye for $B_{68}N_{68}H_{24}$-H^{S1}, respectively. For disclination angle 240˚, the highest surface reactivates for Type1 and Type2 are found to be 12.85 Debye for $B_{47}N_{47}H_{14}$-H^{S2} and 25.20 Debye for $B_{34}N_{34}H_{12}$-H^{S3}, respectively.

Table 8 shows that the surface reactivities for mono-hydrogenated BNNCs-M1-Type1 and BNNCs-M1-Type2 are increased by increasing the cone size and cone angle. For disclination angle 60˚, the highest surface reactivates for Type1 and Type2 are found to be 13.96 Debye for $B_{38}N_{42}H_{20}$-H^{S2} and 10.77 Debye for $B_{83}N_{87}H_{30}$-H^{S1}, respectively. For disclination angle 180˚, the highest surface reactivates for Type1 and Type2 are found to be 20.81 Debye for $B_{68}N_{73}H_{21}$-H^{S1} and 28.50 Debye for $B_{35}N_{40}H_{15}$-H^{S3}, respectively. For disclination angle 300˚, the highest surface reactivates for Type1 and Type2 are found to be 28.97 Debye for $B_{41}N_{49}H_{10}$-H^{S1} and 27.55 Debye for $B_{26}N_{32}H_{8}$-H^{S3}, respectively.

From **Table 9**, it is found that the surface reactivities for mono-hydrogenated BNNCs-M2-Type1 and BNNCs-M2-Type2 are increased by increasing the cone size and cone angle. For disclination angle 60˚, the highest surface reactivates for Type1 and Type2 are found to be 7.44 Debye for $B_{87}N_{83}H_{30}$-H^{S2} and 20.77 Debye for $B_{42}N_{38}H_{20}$-H^{S1}, respectively. For disclination angle 180˚, the highest surface reactivates for Type1 and Type2 are found to be 11.83 Debye and 17.28 Debye $B_{73}N_{68}H_{21}$-H^{S3}, respectively. For disclination angle 300˚, the highest surface reactivates for Type1 and Type2 are found to be 7.26 Debye and 25.94 Debye for $B_{32}N_{26}H_{8}$-H^{S3}, respectively. We can conclude that the best cone size, the best hydrogenation site and best disclination angle for mono-hydrogenated Type1 and Type2 of BNNCs is 28.97 Debye for $B_{41}N_{49}H_{10}$-H^{S1} and 27.55 Debye for $B_{26}N_{32}H_{8}$-H^{S3} at 300˚ declination angle.

Finally, it is found that the surface reactivity for pure and mono-hydrogenated CNCs and BNNCs is increased by increasing the cone angle and the cone size. Also, it is found that the surface reactivity is increased by hydrogenation and the highest surface reactivity is found to be 28.97 Debye for $B_{41}N_{49}H_{10}$-H^{S1} (M1) when the hydrogenation is done on the boron atom (Type1).

Table 7. The configuration structures and the dipole moments of mono-hydrogenated BNNCs-Type1 and BNNCs-Type2 for disclination angles 120˚ and 240˚. The dipole moment is given by Debye.

Angle 120˚			Angle 240˚		
	Dipole moment			Dipole moment	
Systems	Type1	Type2	Systems	Type1	Type2
$B_{18}N_{18}H_{12}$-H^{S1}	4.70	7.66	$B_{14}N_{14}H_{8}$-H^{S1}	3.43	8.22
$B_{18}N_{18}H_{12}$-H^{S2}	6.49	3.45	$B_{14}N_{14}H_{8}$-H^{S2}	5.67	5.67
$B_{18}N_{18}H_{12}$-H^{S3}	5.27	7.98	$B_{14}N_{14}H_{8}$-H^{S3}	5.97	5.81
$B_{28}N_{28}H_{16}$-H^{S1}	5.26	8.34	$B_{23}N_{23}H_{10}$-H^{S1}	5.24	10.13
$B_{28}N_{28}H_{16}$-H^{S2}	7.31	4.61	$B_{23}N_{23}H_{10}$-H^{S2}	8.86	7.69
$B_{28}N_{28}H_{16}$-H^{S3}	5.58	3.72	$B_{23}N_{23}H_{10}$-H^{S3}	7.94	12.64
$B_{46}N_{46}H_{20}$-H^{S1}	7.02	10.09	$B_{34}N_{34}H_{12}$-H^{S1}	7.10	11.97
$B_{46}N_{46}H_{20}$-H^{S2}	9.18	6.12	$B_{34}N_{34}H_{12}$-H^{S2}	10.88	9.60
$B_{46}N_{46}H_{20}$-H^{S3}	7.49	6.84	$B_{34}N_{34}H_{12}$-H^{S3}	10.19	25.20
$B_{68}N_{68}H_{24}$-H^{S1}	8.69	11.75	$B_{47}N_{47}H_{14}$-H^{S1}	8.91	13.92
$B_{68}N_{68}H_{24}$-H^{S2}	10.90	7.60	$B_{47}N_{47}H_{14}$-H^{S2}	12.85	11.45
$B_{68}N_{68}H_{24}$-H^{S3}	9.18	6.81	$B_{47}N_{47}H_{14}$-H^{S3}	11.86	16.77

Table 8. The configuration structures and the dipole moments of mono-hydrogenated BNNCs-M1-Type1 and BNNCs-M1-Type2, for disclination angles 60˚, 180˚ and 300˚. The dipole moment is given by Debye.

Angle 60˚			Angle 180˚			Angle 300˚		
	Dipole moment			Dipole moment			Dipole moment	
Systems	Type1	Type2	Systems	Type1	Type2	Systems	Type1	Type2
$B_{21}N_{24}H_{15}$-H^{S1}	7.20	7.72	$B_{22}N_{26}H_{12}$-H^{S1}	16.37	13.57	$B_{10}N_{13}H_{5}$-H^{S1}	19.05	9.82
$B_{21}N_{24}H_{15}$-H^{S2}	11.07	5.88	$B_{22}N_{26}H_{12}$-H^{S2}	13.65	11.70	$B_{10}N_{13}H_{5}$-H^{S2}	10.19	10.72
$B_{21}N_{24}H_{15}$-H^{S3}	7.01	6.35	$B_{22}N_{26}H_{12}$-H^{S3}	15.68	19.98	$B_{10}N_{13}H_{5}$-H^{S3}	9.04	10.41
$B_{38}N_{42}H_{20}$-H^{S1}	9.47	10.56	$B_{35}N_{40}H_{15}$-H^{S1}	19.83	16.49	$B_{15}N_{19}H_{6}$-H^{S1}	11.06	11.48
$B_{38}N_{42}H_{20}$-H^{S2}	13.90	8.03	$B_{35}N_{40}H_{15}$-H^{S2}	16.63	14.63	$B_{15}N_{19}H_{6}$-H^{S2}	12.56	11.90
$B_{38}N_{42}H_{20}$-H^{S3}	9.49	8.32	$B_{35}N_{40}H_{15}$-H^{S3}	15.28	28.50	$B_{15}N_{19}H_{6}$-H^{S3}	11.95	18.29
$B_{42}N_{56}H_{25}$-H^{S1}	6.73	8.81	$B_{49}N_{53}H_{18}$-H^{S1}	17.78	14.74	$B_{26}N_{32}H_{8}$-H^{S1}	22.92	16.60
$B_{42}N_{56}H_{25}$-H^{S2}	10.80	4.82	$B_{49}N_{53}H_{18}$-H^{S2}	14.10	12.32	$B_{26}N_{32}H_{8}$-H^{S2}	12.03	11.33
$B_{42}N_{56}H_{25}$-H^{S3}	6.90	5.54	$B_{49}N_{53}H_{18}$-H^{S3}	13.10	13.42	$B_{26}N_{32}H_{8}$-H^{S3}	15.56	27.55
$B_{83}N_{87}H_{30}$-H^{S1}	8.87	10.77	$B_{68}N_{73}H_{21}$-H^{S1}	20.81	17.41	$B_{41}N_{49}H_{10}$-H^{S1}	28.97	13.07
$B_{83}N_{87}H_{30}$-H^{S2}	13.18	10.95	$B_{68}N_{73}H_{21}$-H^{S2}	16.97	15.00	$B_{41}N_{49}H_{10}$-H^{S2}	16.79	12.04
$B_{83}N_{87}H_{30}$-H^{S3}	8.96	7.80	$B_{68}N_{73}H_{21}$-H^{S3}	15.90	15.97	$B_{41}N_{49}H_{10}$-H^{S3}	23.17	20.51

Table 9. The configuration structures and the dipole moments of mono-hydrogenated BNNCs-M2-Type1 and BNNCs-M2-Type2, for disclination angles 60˚, 180˚ and 300˚. The dipole moment is given by Debye.

Angle 60˚			Angle 180˚			Angle 300˚		
Systems	Dipole moment		Systems	Dipole moment		Systems	Dipole moment	
	Type1	Type2		Type1	Type2		Type1	Type2
$B_{24}N_{21}H_{15}$-H^{S1}	4.91	17.20	$B_{26}N_{22}H_{12}$-H^{S1}	3.84	8.54	$B_{13}N_{10}H_{5}$-H^{S1}	4.49	3.59
$B_{24}N_{21}H_{15}$-H^{S2}	5.30	10.50	$B_{26}N_{22}H_{12}$-H^{S2}	7.36	8.96	$B_{13}N_{10}H_{5}$-H^{S2}	4.02	2.39
$B_{24}N_{21}H_{15}$-H^{S3}	5.17	4.24	$B_{26}N_{22}H_{12}$-H^{S3}	7.37	17.28	$B_{13}N_{10}H_{5}$-H^{S3}	1.13	8.14
$B_{42}N_{38}H_{20}$-H^{S1}	6.78	20.77	$B_{40}N_{35}H_{15}$-H^{S1}	5.54	10.28	$B_{19}N_{15}H_{6}$-H^{S1}	5.00	3.04
$B_{42}N_{38}H_{20}$-H^{S2}	6.94	12.24	$B_{40}N_{35}H_{15}$-H^{S2}	9.21	10.64	$B_{19}N_{15}H_{6}$-H^{S2}	3.67	7.28
$B_{42}N_{38}H_{20}$-H^{S3}	6.75	20.66	$B_{40}N_{35}H_{15}$-H^{S3}	9.27	14.37	$B_{19}N_{15}H_{6}$-H^{S3}	7.18	13.85
$B_{56}N_{42}H_{25}$-H^{S1}	5.38	16.40	$B_{53}N_{49}H_{18}$-H^{S1}	6.61	12.13	$B_{32}N_{26}H_{8}$-H^{S1}	5.66	4.37
$B_{56}N_{42}H_{25}$-H^{S2}	5.89	9.43	$B_{53}N_{49}H_{18}$-H^{S2}	9.81	9.64	$B_{32}N_{26}H_{8}$-H^{S2}	2.80	3.04
$B_{56}N_{42}H_{25}$-H^{S3}	5.54	10.73	$B_{53}N_{49}H_{18}$-H^{S3}	9.46	15.08	$B_{32}N_{26}H_{8}$-H^{S3}	7.26	25.94
$B_{87}N_{83}H_{30}$-H^{S1}	6.92	9.50	$B_{73}N_{68}H_{21}$-H^{S1}	8.18	13.74	$B_{49}N_{41}H_{10}$-H^{S1}	5.09	8.73
$B_{87}N_{83}H_{30}$-H^{S2}	7.44	11.27	$B_{73}N_{68}H_{21}$-H^{S2}	11.57	11.51	$B_{49}N_{41}H_{10}$-H^{S2}	2.57	4.77
$B_{87}N_{83}H_{30}$-H^{S3}	7.11	7.21	$B_{73}N_{68}H_{21}$-H^{S3}	11.83	11.53	$B_{49}N_{41}H_{10}$-H^{S3}	2.57	14.92

4. Conclusion

The surface reactivity of fifty-two structures of pure CNCs and BNNCs and two hundred and fifty-two structures for mono-hydrogenated CNCs and BNNCs is calculated using density functional (DFT) calculations at the B3LYP/3-21G level of theory. Five disclination angles (60˚, 120˚, 180˚, 240˚ and 300˚), four different nanocone sizes and three different hydrogenation sites are applied. The calculations show that the dipole moments are always increased by increasing the nanocone sizes and the highest surface reactivity for pure CNCs and BNNCs at disclination angles 60˚, 180˚ and 300˚ is 23.50 Debye for $B_{41}N_{49}H_{10}$ cone and at disclination angles 120˚ and 240˚ is 15.30 Debye for $C_{94}H_{14}$ cone. For mono-hydrogenated CNCs, the highest surface reactivity is found 22.17 Debye $C_{90}H_{10}$-H^{S3} at CNC angle 300˚ and for mono-hydrogenated BNNCs the highest surface reactivity is 28.97 Debye for $B_{41}N_{49}H_{10}$-H^{S1} when the hydrogen atom is adsorbed on boron atom at BNNC angle 240˚.

References

[1] Liao, M.L. (2012) Preparation of Ni/Cu Composite Nanowires. *Journal of Nanoparticle Research*, **14**, 837. http://dx.doi.org/10.1007/s11051-012-0837-1

[2] Gotzias, A., Heiberg-Andersen, H., Kainourgiakis, Th. and Steriotis, M. (2011) Study of Hydrogen Adsorption in Nano-Structured Carbon Materials, with a Combination of Experimental Methods and Monte Carlo Simulations. *Carbon*, **49**, 2715-2724. http://dx.doi.org/10.1016/j.carbon.2011.02.062

[3] Mirzaei, M. (2013) Investigating Pristine and Carbon-Decorated Silicon Nanocones: DFT Studies. *Superlattices and Microstructures*, **58**, 130-134. http://dx.doi.org/10.1016/j.spmi.2013.03.007

[4] Esrafili, M.D. and Mahdavinia, G. (2013) Nitrogen-Doped (6,0) and (4,4) Single-Walled SiC Nanotubes: A DFT Study on Surface Reactivity and NMR Parameters. *Superlattices and Microstructures*, **62**, 140-148. http://dx.doi.org/10.1016/j.spmi.2013.07.015

[5] Yu, X. and Raaen, S. (2013) The Influence of Potassium Doping on Hydrogen Adsorption on Carbon Nanocone Material Studied by Thermal Desorption and Photoemission. *Applied Surface Science*, **270**, 364-369. http://dx.doi.org/10.1016/j.apsusc.2013.01.031

[6] Nouri, A. and Mirzaei, M. (2009) A Detailed Theoretical Study of the Interaction of Thiourea with Cis-Diaqua (Ethylenediamine) Platinum(II). *Journal of Molecular Structure*: *THEOCHEM*, **913**, 207-209. http://dx.doi.org/10.1016/j.theochem.2009.07.044

[7] Qu, C.Q., Qiao, L., Wang, C., Yu, S.S., Jiang, Q. and Zheng, W.T. (2010) Experimental and Theoretical Studies on the Magnetic Property of Carbon-Doped ZnO. *Physics Letters A*, **374**, 782-787. http://dx.doi.org/10.1016/j.physleta.2009.11.066

[8] Yu, X., Tverdal, M., Raaen, S., Helgesen, G. and Knudsen, K.D. (2008) Hydrogen Storage in Carbon Cones. *Applied Surface Science*, **255**, 1906-1910. http://dx.doi.org/10.1016/j.apsusc.2008.06.120

[9] Azevedo, S. (2004) Spin Polarization in Carbon Nanostructures with Disclinations. *Physics Letters A*, **325**, 283-286. http://dx.doi.org/10.1016/j.physleta.2004.03.065

[10] Baei, M.T., Peyghan, A.A., Bagheri, Z. and Tabar, M.B. (2012) DFT Study of NH3 Adsorption on Pristine, Ni- and Si-Doped Graphynes. *Physics Letters A*, **377**, 107-111. http://dx.doi.org/10.1016/j.physleta.2012.11.006

[11] Mirzaei, M. and Meskinfam, M. (2011) Computational Studies of Effects of Tubular Lengths on the NMR Properties of Pristine and Carbon Decorated Boron Phosphide Nanotubes. *Solid State Sciences*, **13**, 1926-1930. http://dx.doi.org/10.1016/j.solidstatesciences.2011.08.018

[12] Ge, M. and Sattler, K. (1994) Bundles of Carbon Nanotubes Generated by Vapor-Phase Growth. *Applied Physics Letters*, **64**, 710. http://dx.doi.org/10.1063/1.111042

[13] Ge, M. and Sattler, K. (1994) Observation of Fullerene Cones. *Chemical Physics Letters*, **220**, 192-196. http://dx.doi.org/10.1016/0009-2614(94)00167-7

[14] Merkulov, V.I., Melechko, A.V., Guillom, M.A., Lowndes, D.H. and Simpson, M.L. (2011) Sharpening of Carbon Nanocone Tips during Plasma-Enhanced Chemical Vapor Growth. *Chemical Physics Letters*, **350**, 381-385. http://dx.doi.org/10.1016/S0009-2614(01)01312-4

[15] Shenderova, O.A., Lawson, B.L., Areshkin, D. and Brenner, D.W. (2001) Predicted Structure and Electronic Properties of Individual Carbon Nanocones and Nanostructures Assembled from Nanocones. *Nanotechnology*, **12**, 191. http://dx.doi.org/10.1088/0957-4484/12/3/302

[16] Baylor, L.R., Merkulov, V.I., Ellis, E.D., Guillorn, M.A., Lowndes, D.H., Melechko, A.V., Simpson, M.L. and Whealton, J.H. (2002) Field Emission from Isolated Individual Vertically Aligned Carbon Nanocones. *Journal of Applied Physics*, **91**, 4602-4606. http://dx.doi.org/10.1063/1.1455138

[17] Lu, X., Yang, Q., Xiao, C. and Hirose, A. (2006) Field Electron Emission of Carbon-Based Nanocone Films. *Applied Physics A*, **82**, 293-296. http://dx.doi.org/10.1007/s00339-005-3410-2

[18] Bonard, J.M., Gaal, R., Garaj, S., Thien-Nga, L., Forro, L., Takahashi, K., Kokai, F., Yudasaka, M. and Iijima, S. (2002) Field Emission Properties of Carbon Nanohorn Films. *Journal of Applied Physics*, **91**, Article ID: 10107. http://dx.doi.org/10.1063/1.1481200

[19] Saito, Y., Tsujimoto, Y., Koshio, A. and Kokai, F. (2007) Field Emission Patterns from Multiwall Carbon Nanotubes with a Cone-Shaped Tip. *Applied Physics Letters*, **90**, Article ID: 213108. http://dx.doi.org/10.1063/1.2742637

[20] McGuire, K., Gothard, N., Gai, P.L., Dresselhaus, M.S., Sumanasekera, G. and Rao, A.M. (2005) Synthesis and Raman Characterization of Boron-Doped Single-Walled Carbon Nanotubes. *Carbon*, **43**, 219-227. http://dx.doi.org/10.1016/j.carbon.2004.11.001

[21] Cruz-Silva, E., Cullen, D.A., Gu, L., Romo-Herrera, J.M., Munoz-Sandoval, E., Lopez-Urias, F., Sumpter, B.G., Meunier, V., Charlier, J.C., Smith, D.J., Terrrones, H. and Terrones, M. (2008) Heterodoped Nanotubes: Theory, Synthesis, and Characterization of Phosphorus-Nitrogen Doped Multiwalled Carbon Nanotubes. *ACS Nano*, **2**, 441-448. http://dx.doi.org/10.1021/nn700330w

[22] Terrones, M., Souza, A.G. and Rao, A.M. (2008) Nanostructured Photoelectrodes for Solar Powered Applications. In: Jorio, A., Dresselhaus, G. and Dresselhaus, M.S., Eds., *Carbon Nanotubes*, *Topics in Applied Physics*, Vol. 111, Springer-Verlag, Berlin, 531-566. http://dx.doi.org/10.1007/978-3-540-72865-8_17

[23] Becke, A.D. (1993) Density Functional Thermochemistry. III. The Role of Exact Exchange. *The Journal of Chemical Physics*, **98**, 5648. http://dx.doi.org/10.1063/1.464913

[24] Becke, A.D. (1988) Density-Functional Exchange-Energy Approximation with Correct Asymptotic Behavior. *Physical Review A*, **38**, 3098. http://dx.doi.org/10.1103/PhysRevA.38.3098

[25] Frisch, M.J., Trucks, G.W., Schlegel, H.B., Scuseria, G.E., Robb, M.A., Cheeseman, J.R., Zakrzewski, V.G., Montgomery, J.A., Stratmann, R.E., Burant, J.C., Dapprich, S., Millam, J.M., Daniels, A.D., Kudin, K.N., Strain, M.C., Farkas, O., Tomasi, J., Barone, V., Cossi, M., Cammi, R., Mennucci, B., Pomelli, C., Adamo, C., Clifford, S., Ochterski, J., Petersson, G.A., Ayala, P.Y., Cui, Q., Morokuma, K., Malick, D.K., Rabuck, A.D., Raghavachari, K., Foresman, J.B., Cioslowski, J., Ortiz, J.V., Stefanov, B.B., Liu, G., Liashenko, A., Piskorz, P., Komaromi, I., Gomperts, R., Martin, R.L., Fox, D.J., Keith, T., Al-Lamham, M.A., Peng, C.Y., Nanayakkara, A., Gonzalez, C., Challacombe, M., Gill, P.M.W., Johnson, B.G., Chen, W., Wong, M.W., Andres, J.L., Head-Gordon, M., Replogle, E.S. and Pople, J.A. (2004) Gaussian 2004. Gaussian Inc., Wallingford.

[26] Hindi, A. and EL-Barbary, A.A. (2015) Hydrogen Binding Energy of Halogenated C_{40} Cage: An Intermediate between Physisorption and Chemisorption. *Journal of Molecular Structure*, **1080**, 169-175. http://dx.doi.org/10.1016/j.molstruc.2014.09.034

[27] El-Nahass, M.M., Kamel, M.A., El-Barbary, A.A., El-Mansy, M.A.M. and Ibrahim, M. (2013) FT-IR Spectroscopic Analyses of 3-Methyl-5-Pyrazolone (MP). *Spectrochimica Acta Part A: Molecular and Biomolecular Spectroscopy*, **111**, 37-41. http://dx.doi.org/10.1016/j.saa.2013.03.072

[28] Kotz, J.C., Treichel, P. and Weaver, G.C. (2006) Chemistry and Chemical Reactivity. Thomson Brooks/Cole, Pacific Grove.